

Global textures and the Doppler peaks

Alejandro Gangui¹

ICTP – International Center for Theoretical Physics, Trieste, Italy

Ruth Durrer and Mairi Sakellariadou

Dépt de Physique Théorique, Université de Genève, Switzerland

Abstract. We review recent work aimed at showing how global topological defects influence the shape of the angular power spectrum of the cosmic microwave background radiation on small scales. While Sachs–Wolfe fluctuations give the dominant contribution on angular scales larger than about a few degrees, on intermediate scales, $0.1^\circ \lesssim \theta \lesssim 2^\circ$, the main rôle is played by coherent oscillations in the baryon radiation plasma before recombination. In standard cosmological models these oscillations lead to the ‘Doppler peaks’ in the angular power spectrum. Inflation–based cold dark matter models predict the location of the first peak to be at $\ell \sim 220/\sqrt{\Omega_0}$, with a height which is a few times the level of anisotropies at large scales. Here we focus on perturbations induced by global textures. We find that the height of the first peak is reduced and is shifted to $\ell \sim 350$.

1. Introduction

The importance of the observations of anisotropies on intermediate and small angular scales cannot be over-emphasized. Presently a number of experiments scrutinize different regions of the sky trying to uncover the real amplitude and structure of the relic radiation. The CMB anisotropies are a powerful tool to discriminate among the different models of structure formation by purely linear analysis. These anisotropies are parameterized in terms of C_ℓ ’s, defined as the coefficients in the expansion of the angular correlation function

$$\langle C_2(\vartheta) \rangle = \frac{1}{4\pi} \sum_{\ell} (2\ell + 1) C_\ell P_\ell(\cos \vartheta). \quad (1)$$

For Harrison–Zel’dovich spectra of perturbations $\ell(\ell + 1)C_\ell$ is constant on large angular scales, say $\ell \lesssim 50$. Both inflation and topological defect models lead to approximately scale invariant spectra on large scales. The next important step towards discriminating between competing models is the measurement of

¹Also at *SISSA – International School for Advanced Studies*, gangui@gandalf.sissa.it

degree scale anisotropies. Disregarding Silk damping, gauge invariant linear perturbation analysis leads to (Durrer 1994)

$$\frac{\delta T}{T} = \left[-\frac{1}{4}D_g^{(r)} + V_j\gamma^j - \Psi + \Phi \right]_i^f + \int_i^f (\Psi' - \Phi')d\tau, \quad (2)$$

where Φ and Ψ are quantities describing the perturbations in the geometry and \mathbf{V} denotes the peculiar velocity of the radiation fluid with respect to the overall Friedmann expansion. In Eq.(2), $D_g^{(r)} = \delta\rho_r/\rho_r$ specifies the intrinsic density fluctuation in the radiation fluid; below we use $D_r = (\delta\rho_r + \delta\rho_b)/(\rho_r + \rho_b)$, about 5% smaller than $D_g^{(r)}$ for scales inside the horizon, which are the ones we are interested in.

The Sachs–Wolfe (SW) contribution in the above equation has been calculated for both inflation and defect models, yielding mainly a normalization of the spectra. We present below a computation for the Doppler contribution from global topological defects; in particular we perform our analysis for π_3 -defects, textures (Turok 1989), in a universe dominated by cold dark matter (CDM). We believe that the main ideas of our analysis remain valid for all global defects. The Doppler contribution to the CMB anisotropies is approximately given by¹

$$\left[\frac{\delta T}{T}(\vec{x}, \hat{\gamma}) \right]^{Doppler} \approx \frac{1}{4}D_r(\vec{x}_{rec}, \eta_{rec}) - \vec{V}(\vec{x}_{rec}, \eta_{rec}) \cdot \hat{\gamma}, \quad (3)$$

where $\vec{x}_{rec} = \vec{x} + \hat{\gamma}\eta_0$. In the previous formula $\hat{\gamma}$ denotes a direction in the sky and η is the conformal time, with η_0 and η_{rec} the present and recombination times, respectively.

2. Linear theory power spectra

We now study a two–fluid system: baryons plus radiation, which prior to recombination are tightly coupled, and CDM. We start off by considering the evolution equations in each fluid component as given by Kodama & Sasaki (1984). The evolution of the perturbation variables in a flat background, $\Omega = 1$, can be expressed as

$$\begin{aligned} V_r' + \frac{a'}{a}V_r &= k\Psi + k\frac{c_s^2}{1+w}D_r \\ V_c' + \frac{a'}{a}V_c &= k\Psi \\ D_r' - 3w\frac{a'}{a}D_r &= (1+w)[3\frac{a'}{a}\Psi - 3\Phi' - kV_r - \frac{9}{2}\left(\frac{a'}{a}\right)^2 k^{-1}(1 + \frac{w\rho_r}{\rho})V_r] \\ D_c' &= 3\frac{a'}{a}\Psi - 3\Phi' - kV_c - \frac{9}{2}\left(\frac{a'}{a}\right)^2 k^{-1}(1 + \frac{w\rho_r}{\rho})V_c, \end{aligned} \quad (4)$$

where subscripts r and c denote the baryon–radiation plasma and CDM, respectively; D , V are density and velocity perturbations; $w = p_r/\rho_r$, $c_s^2 = p_r'/\rho_r'$ and $\rho = \rho_r + \rho_c$.

¹We are neglecting here the SW effect, which decays on subhorizon scales like ℓ^{-2} . We also neglect the contribution of the neutrino fluctuations. These approximations lead to an error of less than about 30% in the amplitude of the first Doppler peak; see discussion in (Durrer, Gangui & Sakellariadou 1995).

Throughout this section we will normalize the scale factor such that $a(\eta_{eq}) = 1$, where η_{eq} is the conformal time at which matter and radiation densities coincide. Setting $\tau \equiv (8\pi G\rho_{eq}/6)^{-1/2}$, where ρ_{eq} is the total energy density at equality, we obtain $a(\eta) = (\eta/\tau)(1 + \frac{1}{4}(\eta/\tau))$. It is clear from this expression that for early (late) conformal times we recover the radiation (matter) dominated phase of expansion of the universe.

Since the energy density of baryons and CDM go like $\propto a^{-3}$, the ratio ρ_B/ρ_c is const and equal to Ω_B . Therefore $(\rho_B/\rho_{rad}) \simeq \Omega_B a$. This leads to

$$w \simeq \frac{1}{3}(1 + \Omega_B a)^{-1} \quad ; \quad c_s^2 \simeq \frac{1}{3}(1 + \frac{3}{4}\Omega_B a)^{-1}. \quad (5)$$

The only place where the seeds enter the system (4) is through the potentials Ψ and Φ . These potentials may be split into a part coming from standard matter and radiation, and a part due to the seeds, e.g., $\Psi = \Psi_{(c,r)} + \Psi_{seed}$ where Ψ_{seed}, Φ_{seed} are determined by the energy momentum tensor of the seed; the global texture in our case. Having said this, one may easily see how the seed source terms arise. Long but straightforward algebra leads to two second order equations for D_r and D_c , namely

$$\begin{aligned} D_r'' + \frac{a'}{a}[1 + 3c_s^2 - 6w + F^{-1}\rho_c]D_r' - \frac{a'}{a}\rho_c F^{-1}(1+w)D_c' \\ + 4\pi G a^2[\rho_r(3w^2 - 8w + 6c_s^2 - 1) - 2F^{-1}w\rho_c(\rho_r + \rho_c) \\ + \rho_c(9c_s^2 - 7w) + \frac{k^2}{4\pi G a^2}c_s^2]D_r - 4\pi G a^2\rho_c(1+w)D_c = (1+w)S ; \\ D_c'' + \frac{a'}{a}[1 + (1+w)F^{-1}\rho_r(1 + 3c_s^2)]D_c' - \frac{a'}{a}(1 + 3c_s^2)F^{-1}\rho_r D_r' \\ - 4\pi G a^2\rho_c D_c - 4\pi G a^2\rho_r(1 + 3c_s^2)[1 - 2(\rho_r + \rho_c)F^{-1}w]D_r = S , \end{aligned} \quad (6)$$

where $F \equiv k^2(12\pi G a^2)^{-1} + \rho_r(1+w) + \rho_c$ and S denotes a source term, which in general is given by $S = 4\pi G a^2(\rho + 3p)^{seed}$. In our case, where the seed is described by a global scalar field ϕ , we have $S = 8\pi G(\phi')^2$. From numerical simulations one finds that the average of $|\phi'|^2$ over a shell of radius k , can be modeled by (Durrer & Zhou 1995)

$$\langle |\phi'|^2 \rangle(k, \eta) = \frac{\frac{1}{2}A\tilde{\eta}^2}{\sqrt{\tilde{\eta}[1 + \alpha(k\eta) + \beta(k\eta)^2]}}, \quad (7)$$

with $\tilde{\eta}$ denoting the symmetry breaking scale of the phase transition leading to texture formation. The parameters in (7) are $A \sim 3.3$, $\alpha \sim -0.7/(2\pi)$ and $\beta \sim 0.7/(2\pi)^2$. On super-horizon scales, where the source term is important, this fit is accurate to about 10%. On small scales the accuracy reduces to a factor of 2. By using this fit in the calculation of D_r and D_c from Eqs.(6) we effectively neglect the time evolution of phases of $(\phi')^2$; the incoherent evolution of these phases may smear out subsequent Doppler peaks (Albrech et al. 1995), but will not affect substantially the height of the first peak.

3. Choosing initial conditions

In defect models of large scale structure formation one usually assumes that the universe begins in a hot, homogeneous state. All perturbation variables are zero, and the primordial fields (e.g., the global field ϕ in our case) are in thermal equilibrium in the unbroken symmetry phase. When the phase transition occurs the original value $\phi = 0$ becomes unstable and ϕ assumes a value which lies in the sphere of degenerate minima determined by $\langle \phi^2 \rangle = \tilde{\eta}^2$. Causality requires the correlation length to be bounded by the size of the horizon. On super-horizon scales the correlations vanish and therefore the defect stress energy tensor has a white noise power spectrum for $k\eta \ll 1$. After the phase transition, the defect energy rapidly enters scaling, $\rho_{def} \propto \eta^{-2}$. Adopting this white noise behaviour of the field on super-horizon scales, one can simulate ϕ on scales much larger than the horizon scale at the phase transition. The only condition is that the scales considered are super-horizon at the time one starts the simulation. This is very important, since the scales relevant for large scale structure are more than 50 orders of magnitude larger than the inverse symmetry breaking scale $\tilde{\eta}^{-1}$.

Going back now to our set of Eqs.(6) we will specify our initial conditions as follows: for a given scale k we choose the initial time η_{in} such that the perturbation is super-horizon and the universe is radiation dominated. In this limit the evolution equations reduce to

$$D_r'' - \frac{2}{\eta^2} D_r' = \frac{4}{3} \frac{A\epsilon}{\sqrt{\eta}} \quad ; \quad D_c'' + \frac{3}{\eta} D_c' - \frac{3}{2\eta} D_r' - \frac{3}{2\eta^2} D_r = \frac{A\epsilon}{\sqrt{\eta}}, \quad (8)$$

with particular solutions $D_r = -\frac{16}{15}\epsilon A\eta^{3/2}$ and $D_c = -\frac{4}{7}\epsilon A\eta^{3/2}$. In the above equations we have introduced $\epsilon \equiv 4\pi G\tilde{\eta}^2$, the only free parameter in the model. We consider perturbations seeded by the texture field, and therefore it is incorrect to add a homogeneous growing mode to the above solutions. With these initial conditions, Eqs.(6) are easily integrated numerically, leading to the spectra for $D_r(k, \eta_{rec})$ and $D_r'(k, \eta_{rec})$. (see Durrer, Gangui & Sakellariadou 1995 for details).

4. Angular power spectrum from global textures

In this section we calculate the expression for C_ℓ as a function of the baryon-radiation power spectrum and its derivative, evaluated at recombination, η_{rec} . We express the Fourier transform of the velocity perturbation in the baryon-radiation component as $\vec{V}(\vec{k}) \simeq -i\vec{k}D_r'(\vec{k})/[k^2(1+w)]$. We then Fourier transform the Doppler contribution to the anisotropies given by Eq.(3) and perform a standard analysis to get the Doppler contribution to the angular power spectrum C_ℓ . This is given as a function of the spectra for $D_r(k, \eta_{rec})$ and $D_r'(k, \eta_{rec})$ as follows

$$C_\ell = \frac{2}{\pi} \int dk \left[\frac{k^2}{16} |D_r(k, t_{rec})|^2 j_\ell^2(kt_0) + (1+w)^{-2} |D_r'(k, t_{rec})|^2 (j_\ell'(kt_0))^2 \right]. \quad (9)$$

As we mentioned earlier, the source term in Eqs.(6) was estimated from numerical simulations of the evolution of the defect field, which give a fit for the

Doppler peaks from global textures

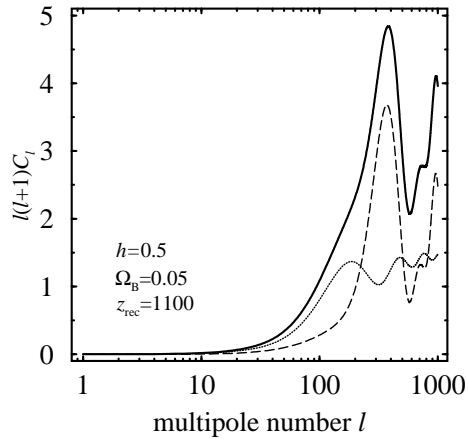


Figure 1. The angular power spectrum for the Doppler contribution to the CMB anisotropies is shown in units of ϵ^2 (thick solid curve). Contributions from the baryon–radiation density perturbation (dashed curve) and its derivative (dotted curve) from Eq.(9) are also shown.

absolute value of ϕ , but do not specify the phases. The crossed term missing in Eq.(9), cannot be determined with this method. However, due to phase averaging, we expect it to be diminished substantially and therefore we neglect it. Integrating Eq.(9), we obtain the Doppler contribution to the CMB anisotropies shown in Figure 1.

5. Discussion

As we see from the figure, the angular power spectrum $\ell(\ell + 1)C_\ell$ yields the Doppler peaks. For $\ell < 1000$, we find three peaks located at $\ell = 365$, $\ell = 720$ and $\ell = 950$. Silk damping, which we have not taken into account here, will decrease the relative amplitude of the third peak with respect to the second one; however it will not affect substantially the height of the first peak. The integrated SW effect, which also has been neglected, will shift the position of the first peak to somewhat larger scales, lowering ℓ_{peak} by (5 – 10)% and possibly increasing its amplitude slightly (by less than 30%) (Durrer, Gangui & Sakellariadou 1995).

Our second important result regards the amplitude of the first Doppler peak, for which we find $\ell(\ell + 1)C_\ell|_{\ell \sim 365} = 5\epsilon^2$. It is interesting to notice that the position of the first peak is displaced by $\Delta\ell \sim 150$ towards smaller angular scales than in standard inflationary models (Steinhardt 1995). This is due to the difference in the growth of super–horizon perturbations (Sugiyama 1996), which is $D_r \propto \eta^{3/2}$ in our case, and $D_r \propto \eta^2$ for inflationary models.

Let us now compare our value for the Doppler peak with the level of the SW plateau. Unfortunately the numerical value for the SW amplitude is uncertain within a factor of about 2, which leads to a factor 4 uncertainty in the SW contribution to the power spectrum: the results are $\ell(\ell + 1)C_\ell|_{SW} \sim 2\epsilon^2$ (Ben-

nett & Rhie 1993; Pen et al. 1994) and $\ell(\ell + 1)C_\ell|_{sw} \sim 8\epsilon^2$ (Durrer & Zhou 1995). According to the first two groups, the Doppler peak is a factor of ~ 3.4 times higher than the SW plateau, whereas it is only about 1.5 times higher if the second result is assumed. (We allow for about 30% of the SW amplitude to be added in phase to the Doppler amplitude of $\sim 2.24\epsilon$.) Improved numerical simulations or analytical approximations are needed to resolve this discrepancy. However, it is apparent that the Doppler contribution from textures is somewhat smaller than for generic inflationary models.

We believe that our results, about the position and amplitude of the first Doppler peak, are basically valid for all global defects. This depends crucially on the $1/\sqrt{\eta}$ behavior of $(\phi')^2$ on large scales (cf. Eq. (7)). The displacement of the peaks towards smaller scales is reminiscent of open models, where the first Doppler peak is located at $\ell_{peak} \simeq 220/\sqrt{\Omega_0}$. A value $\Omega_0 \simeq 0.3$ would produce $\ell_{peak} \simeq 365$ for the first peak, as we actually find. However, the amplitude of the peaks within open inflationary models is generically larger than the one we find for global defects.

The problem treated in this paper has also been studied by (Crittenden & Turok 1995). They obtained the same position of the first Doppler peak but with a somewhat higher amplitude.

Acknowledgments. One of us (A.G.) is grateful to the organizers of the meeting for the invitation to present the seminar. A.G. thanks the ICTP and the British Council for partial financial support.

References

- Albrecht, A. et al., astro-ph/9505030.
 Bennett, D. & Rhie, S.H. 1993, *Astrophys. J.* **406**, L7.
 Crittenden, R.G. & Turok, N. 1995, *Phys. Rev. Lett.* **75**, 2642.
 Durrer, R. 1994, *Fund. of Cosmic Physics* **15**, 209.
 Durrer, R., Gangui, A. & Sakellariadou, M. 1995, submitted to *Phys.Rev.Lett.*
 Durrer, R. & Zhou, Z.H. 1995, astro-ph/9508016.
 Kodama, H. & Sasaki, M. 1984, *Prog. Theor. Phys. Suppl.* **78**, 1.
 Pen, U.-L., Spergel, D.N. & Turok, N. 1994, *Phys. Rev.* **D49**, 692.
 Steinhardt, P.J. 1995, ‘Cosmology at the Crossroads’, astro-ph/9502024.
 Sugiyama, N. 1996, these proceedings.
 Turok, N. 1989, *Phys. Rev. Lett.* **63**, 2625.